Electronic Supplementary Information

Truncated octahedra $NaCe(MoO_4)_2$ nanostructure: a potential material for blue emission and acetone sensing

Nibedita Haldar,[(a)#] Tanmoy Mondal[(a)], Tanushri Das[(a, b)], Debabrata Sarkar[(c)], Mrinal Pal[(b)], Asiful H. Seikh[(d)] and Chandan Kumar Ghosh[(a)*]

[(a)]School of Materials Science and Nanotechnology, Jadavpur University, Jadavpur, Kolkata – 700032, India

[(b)]CSIR-Central Glass and Ceramic Research Institute, Kolkata – 700032

[(c)]Applied NanoPhysics Laboratory, Department of Physics and Nanotechnology, SRM Institute of Science and Technology, Kattankulathur – 603203, India

[(d)]Mechanical Engineering Department, College of Engineering, King Saud University, Riyadh, 11421, Saudi Arabia

[#] At present: University of Engineering and Management, New Town, Kolkata - 700160

[*]Corresponding author's email ID: chandan.kghosh@jadavpuruniversity.in, Tel: 033-2457-3028

Table S1 Refined structural parameters and the reliability factors from the Rietveld fitting of NCMO samples.

Properties		$NCMO_{0.00}$	$NCMO_{0.50}$	$NCMO_{0.78}$	$NCMO_{1.00}$
Lattice parameter (A^0)	a=b	5.412(8)	5.404(2)	5.404(2)	5.398(9)
	c	11.569(2)	11.487(5)	11.478(5)	11.440(4)
Unit cell volume $(A^0)^3$		338.931(1)	335.755(3)	335.209(2)	333.518(2)
Bond length (A^0)	Na/Ce-O	2.514(3) 2.374(8)	2.497(4) 2.306(2)	2.467(8) 2.276(2)	2.448(4) 2.257(8)
	Mo-O	1.772(1)	1.784(5)	1.786(5)	1.789(5)
Bond angle (in degree)	Na/Ce-O-Na/Ce	102.842(4)	102.033(10)	101.996(9)	102.008(9)
	Na/Ce-O-Mo	133.820(3)	133.244(7)	133.238(7)	133.226(6)
	O-Mo-O	107.397(4)	106.587(10)	106.550(9)	106.532(9)
Crystallite size (nm)		71.20	92.00	107.70	91.40
R_p (%)		14.10	12.10	16.20	15.00
R_{wp} (%)		18.80	18.20	17.60	18.40
R_{exp} (%)		8.77	14.60	13.40	10.80
χ^2		3.57	2.29	3.53	3.29

Table S2 Calculated energy (from DFT) for Acetone adsorption of NCMO samples.

System	$E_{NCMO + acetone}$ (eV)	E_{NCMO} (eV)	$E_{acetone}$ (eV)	E_{ads} (eV)	No of atom (NCMO + acetone)	E_{ads} (eV)/atom
NCMO	-195.666	-97.069	67.592	-166.189	33	-5.030
NCMO – $V_O^{\bullet}$	-186.202	-87.194	67.592	-166.600	32	-5.206
NCMO – $2V_O^{\bullet}$	-196.614	-77.141	67.592	-187.065	31	-6.030

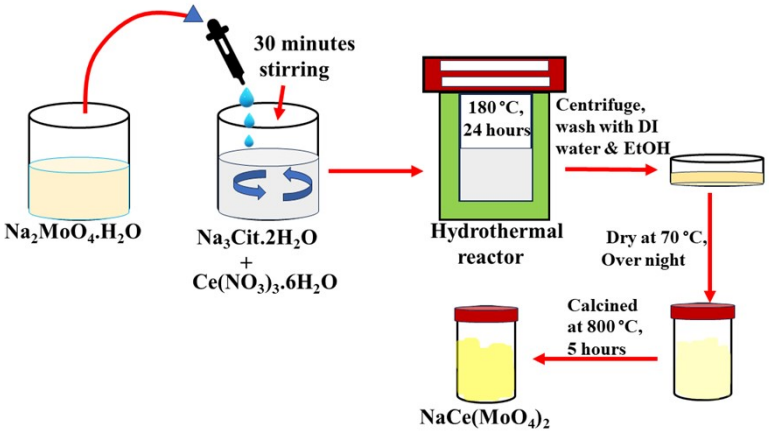

Fig. S1 Schematic representation of reaction procedure.

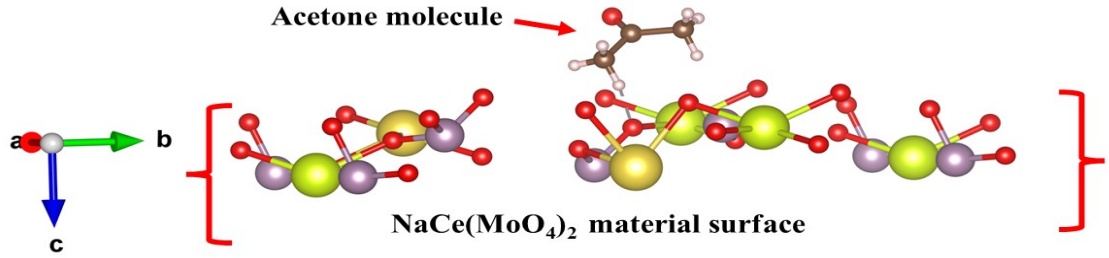

Fig. S2 Atomic structure of acetone molecule adsorption on NCMO (112) surface.

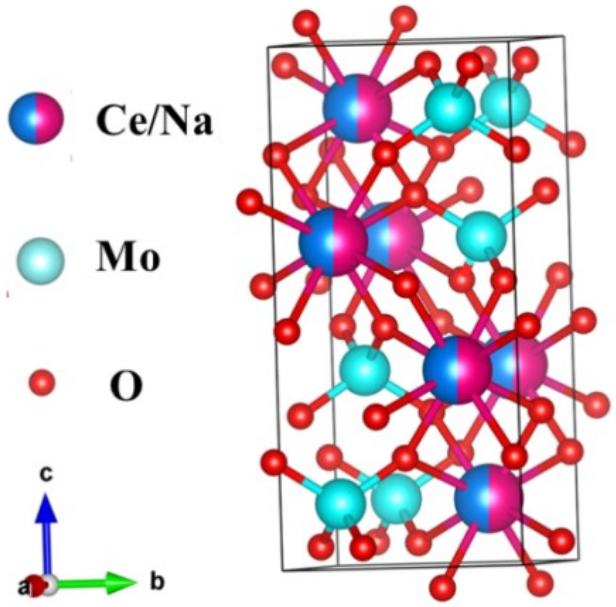

Fig. S3 Structure of the NCMO (Tetragonal) nanostructure.

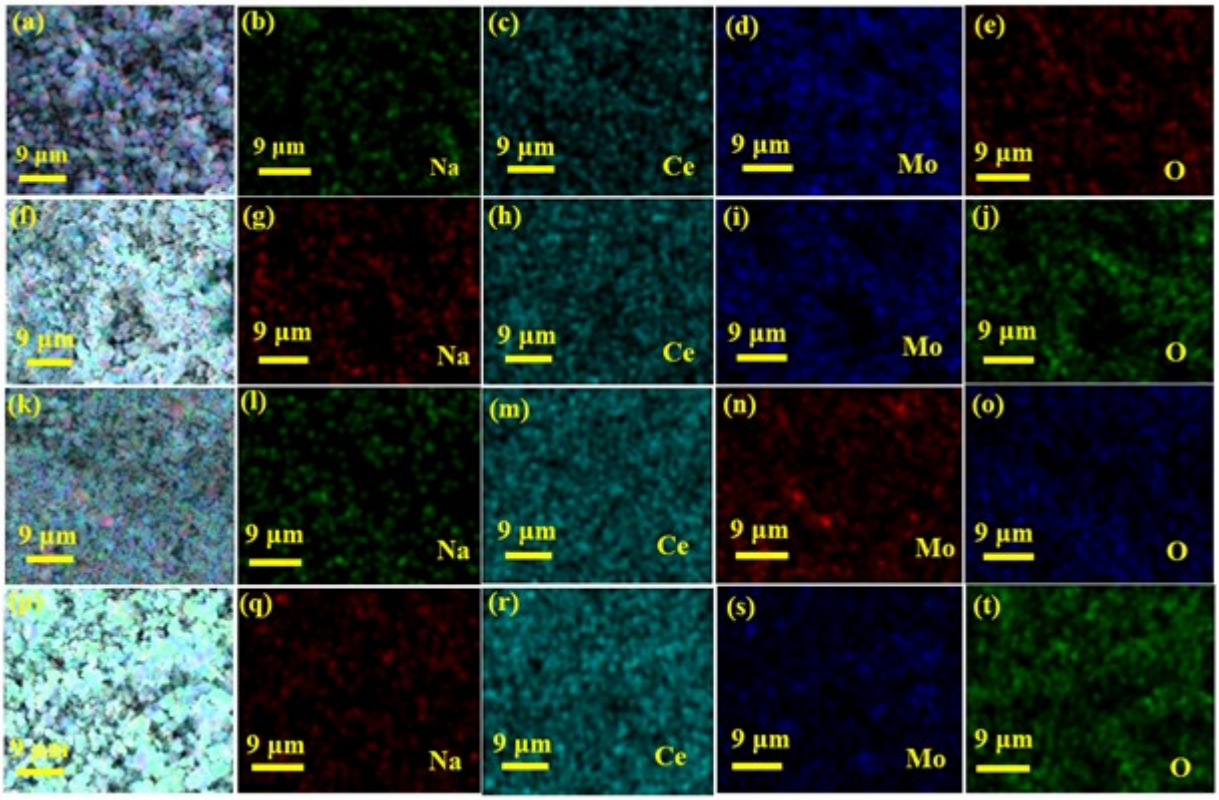

Fig S4 Elemental mapping of $^{NCMO}_{0.00}$ ((a) – (e)), $^{NCMO}_{0.50}$ ((f)) – (j)), $^{NCMO}_{0.78}$ ((k) – (o)) and $^{NCMO}_{1.00}$ ((p) – (t)) respectively.

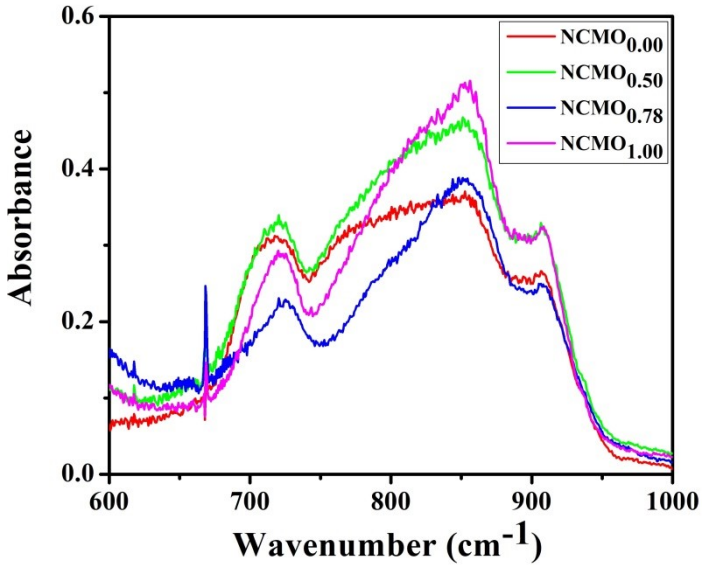

Fig. S5 FTIR spectra of NCMO nanostructures.

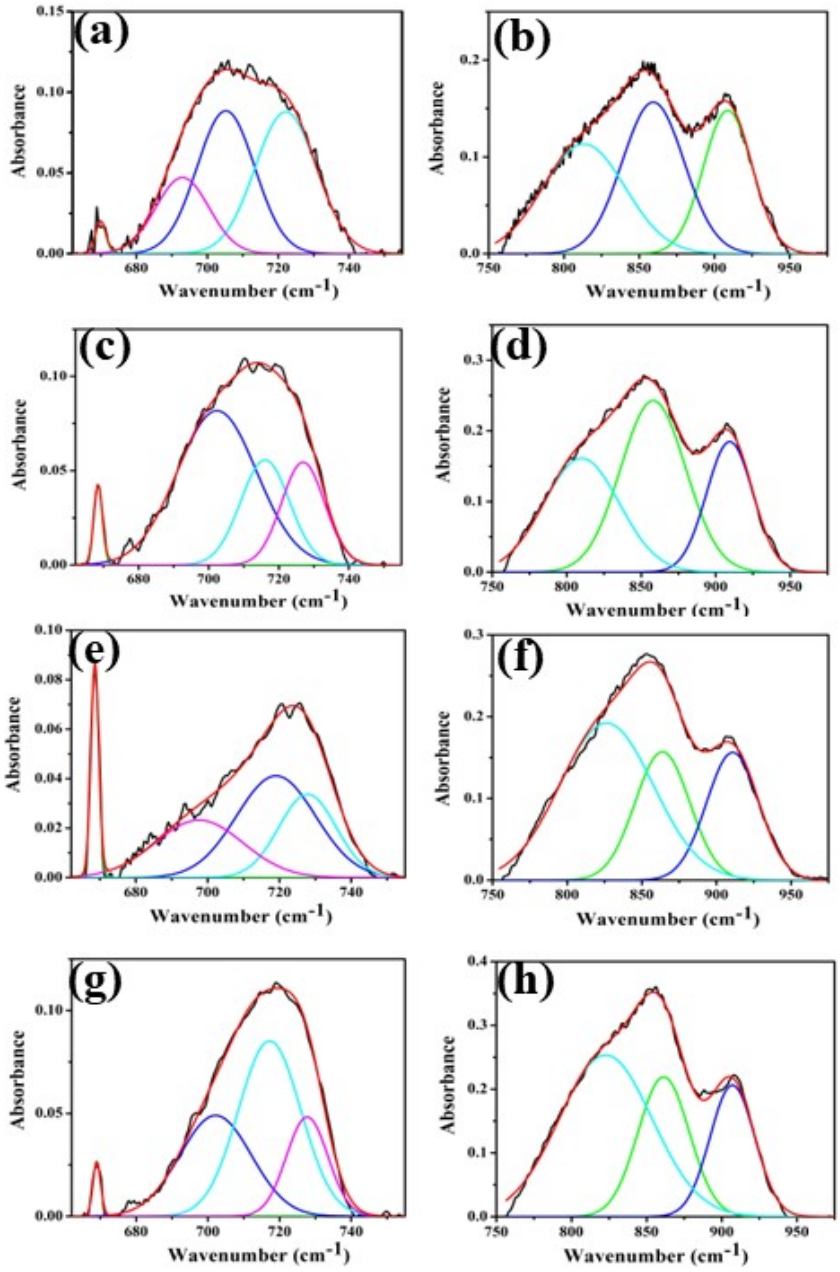

Fig. S6 Deconvoluted FTIR bands 660-750 and 750-960 of $NCMO_{0.00}$ (a, b), $NCMO_{0.50}$ (c, d), $NCMO_{0.78}$ (e, f) and $NCMO_{1.00}$ (g, h) respectively.

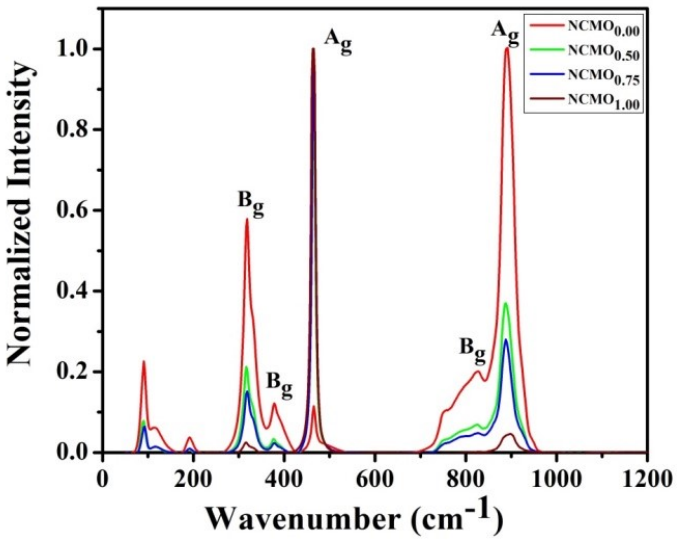

Fig. S7 Raman spectra of NCMO nanostructures.

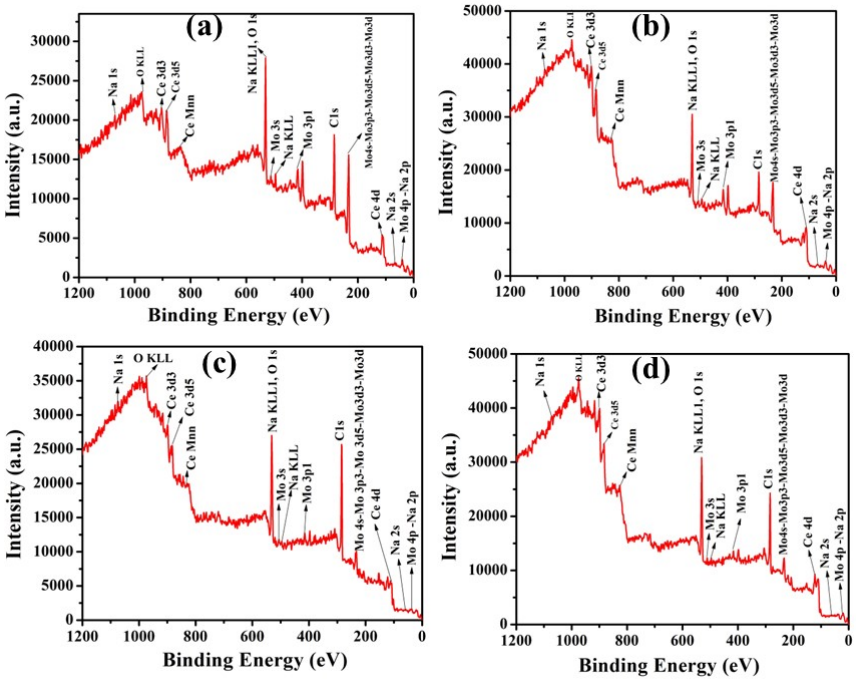

Fig. S8 XPS wide spectrum of Ce-3d, W-4f, O-1s, Na-1s of (a) $NCMO_{0.00}$, (b) $NCMO_{0.50}$, (c) $NCMO_{0.78}$ and (d) $NCMO_{1.00}$ respectively.

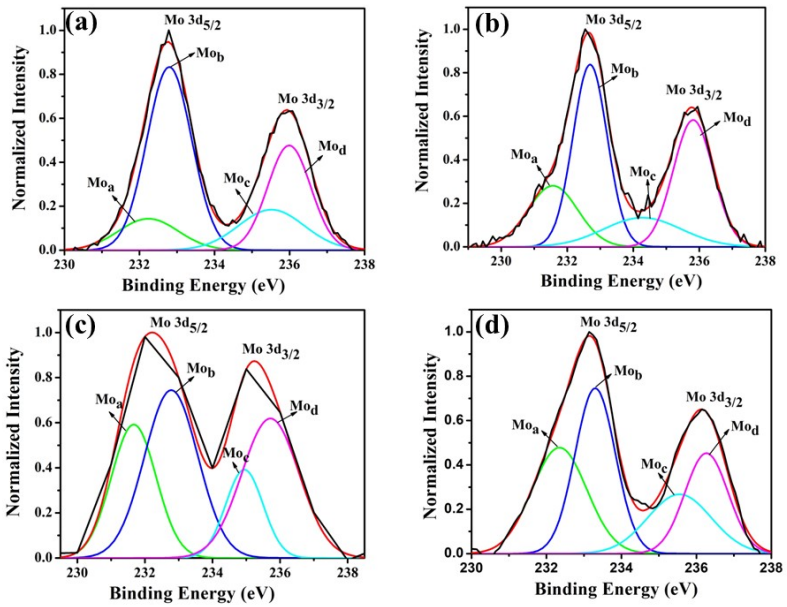

Fig. S9 XPS Mo 3d of (a) $NCMO_{0.00}$, (b) $NCMO_{0.50}$, (c) $NCMO_{0.78}$ and (d) $NCMO_{1.00}$ respectively.

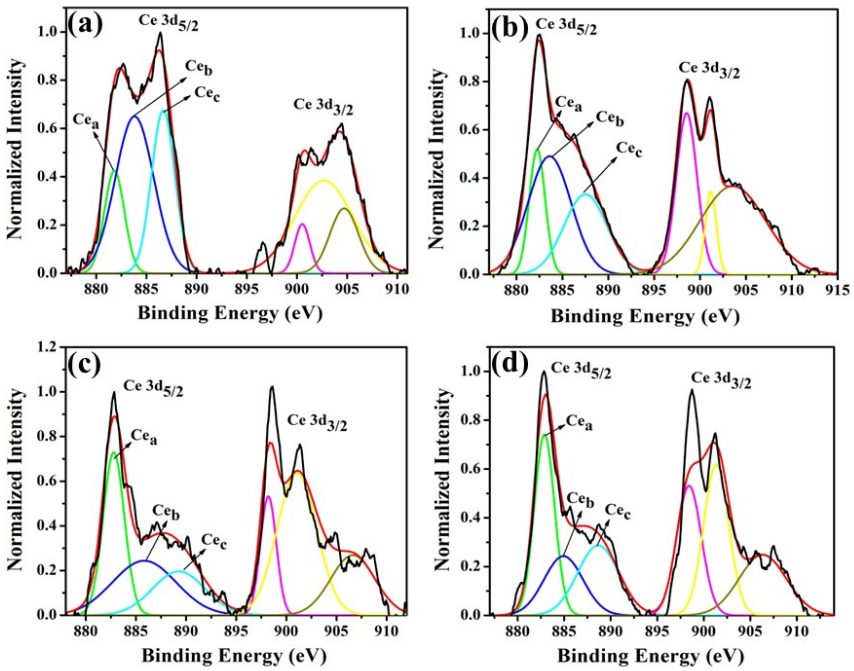

Fig. S10 XPS Ce 3d core level spectra of (a) $NCMO_{0.00}$, (b) $NCMO_{0.50}$, (c) $NCMO_{0.78}$ and (d) $NCMO_{1.00}$ respectively.

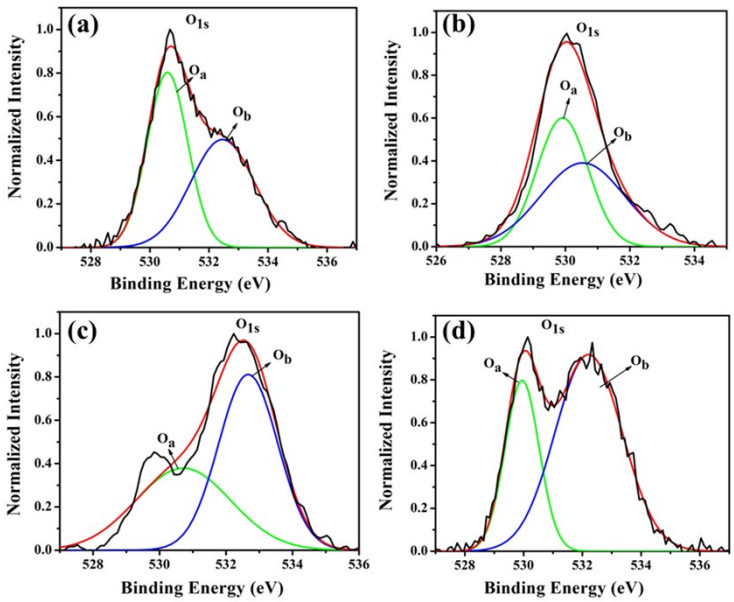

Fig. S11 XPS O1s core level spectra of (a) $NCMO_{0.00}$, (b) $NCMO_{0.50}$, (c) $NCMO_{0.78}$ and (d) $NCMO_{1.00}$ respectively.

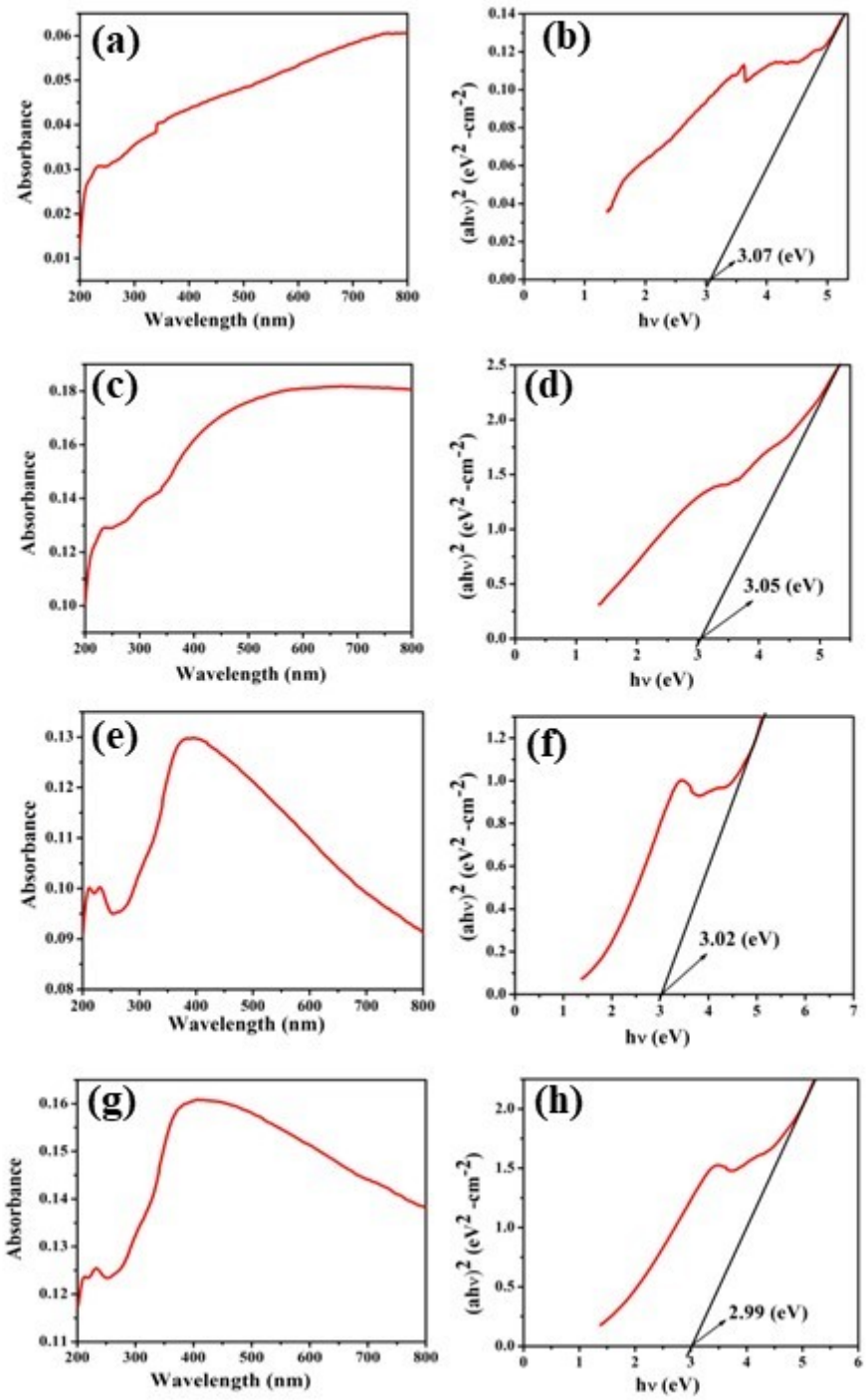

Fig. S12 UV spectra and corresponding band gap of (a, b) $NCMO_{0.00}$, (c, d) $NCMO_{0.50}$, (e, f) $NCMO_{0.78}$ and (g, h) $NCMO_{1.00}$ respectively.

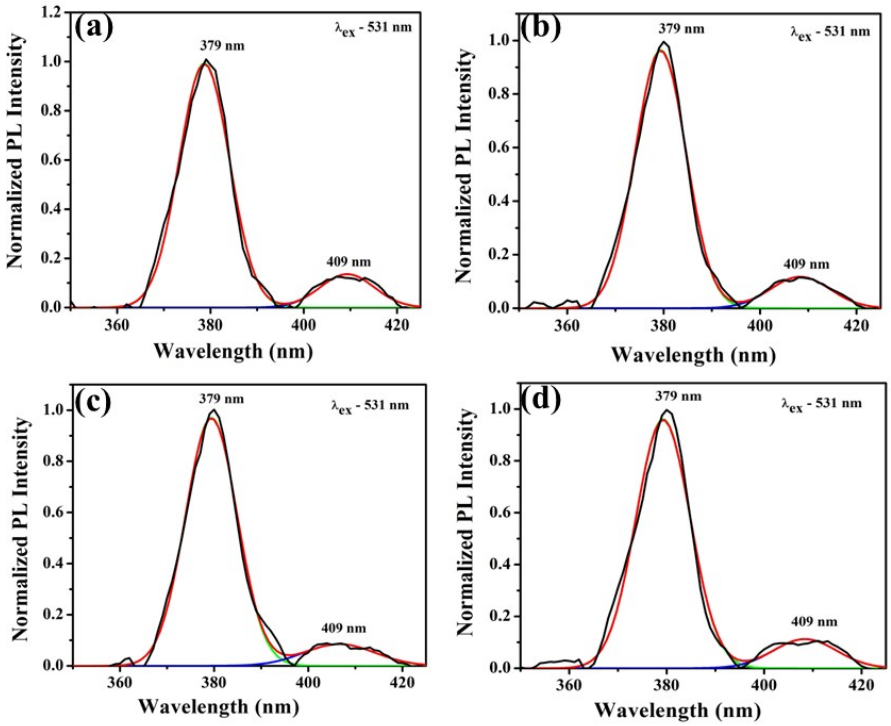

Fig. S13 PLE spectra of (a) $NCMO_{0.00}$, (b) $NCMO_{0.50}$, (c) $NCMO_{0.78}$ and (d) $NCMO_{1.00}$ respectively.

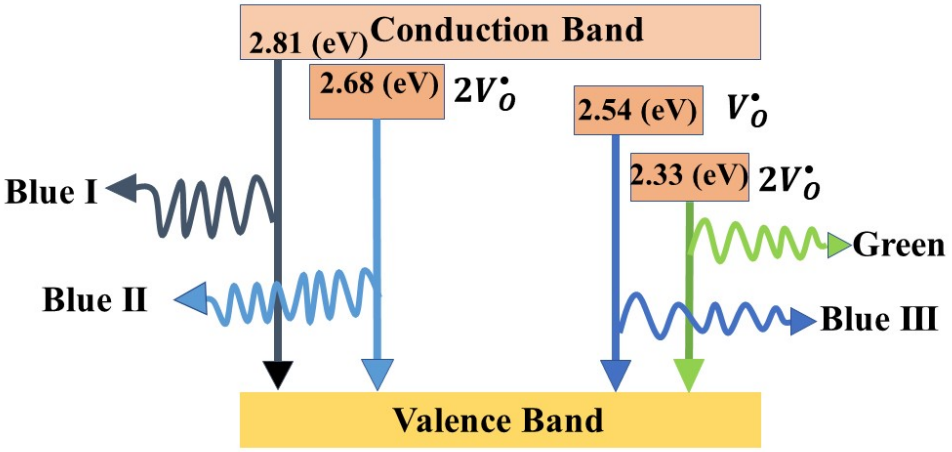

Fig. S14 Schematic representation of luminescent transitions of NCMO.

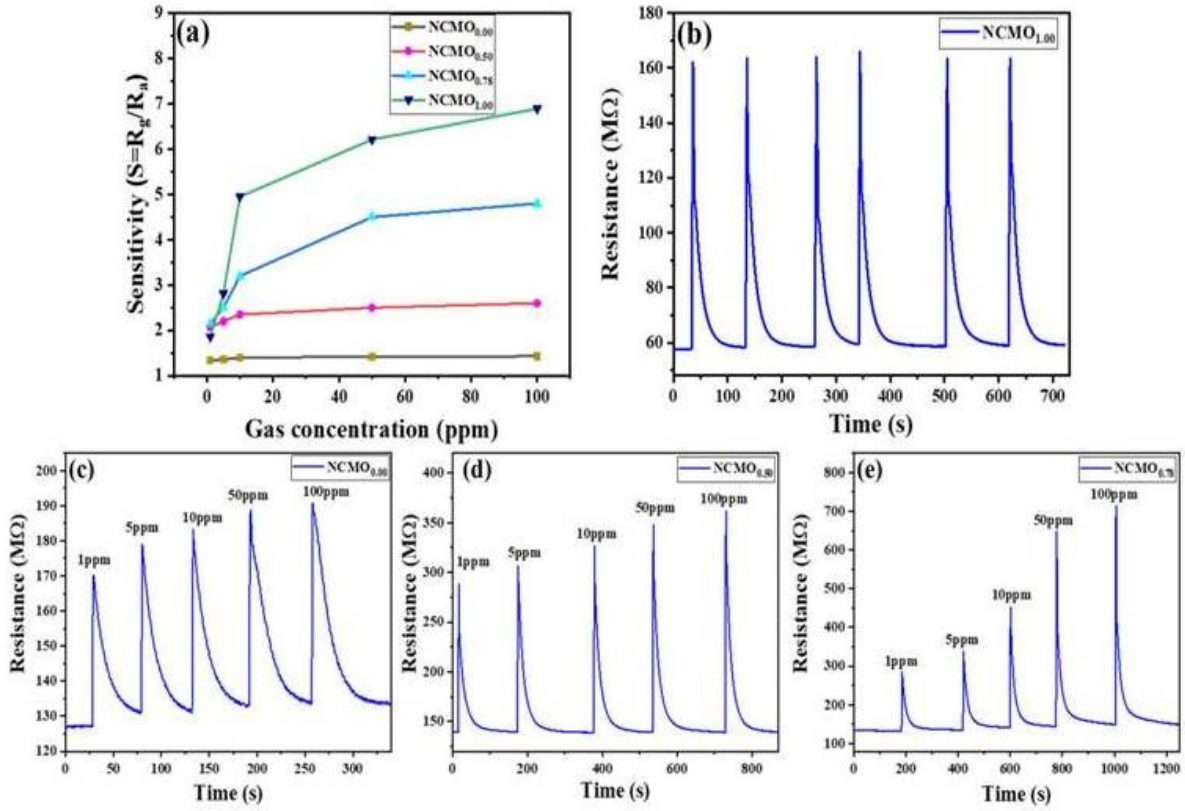

Fig. S15 (a) Sensitivity vs acetone concentration (1-100 ppm) curve for $NCMO_{0.00}$, $NCMO_{0.50}$, $NCMO_{0.78}$ and $NCMO_{1.00}$ at 300°C, (b) Cyclic response-recovery curves of $NCMO_{1.00}$ sensor to 5 ppm acetone for six consecutive cycles of measurement at 300°C. Dynamic acetone response curve of (c) $NCMO_{0.00}$, (d) $NCMO_{0.50}$ and (e) $NCMO_{0.78}$ sensor to acetone concentration from 1 – 100 ppm at 300°C, respectively.

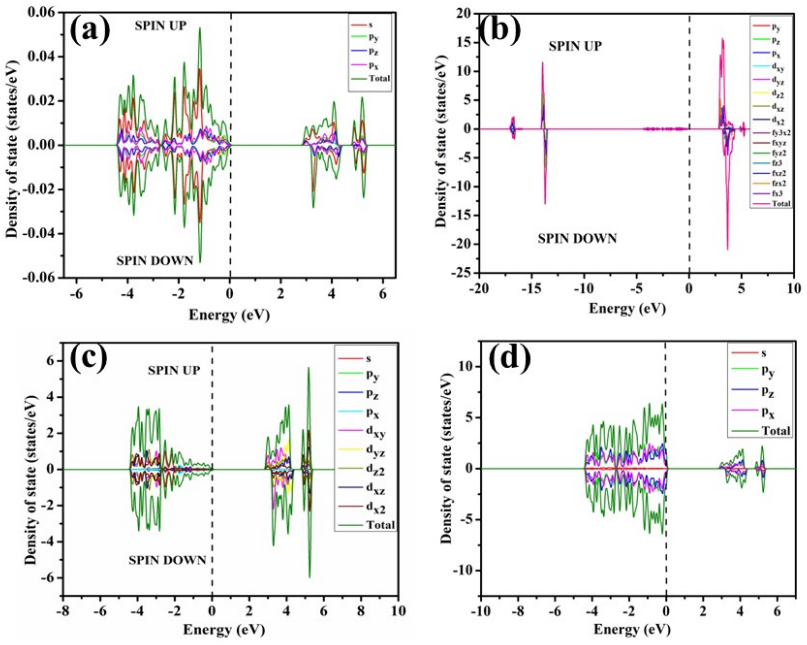

Fig. S16 PDOS of (a) Na, (b) Ce, (c) Mo and (d) O of NCMO.

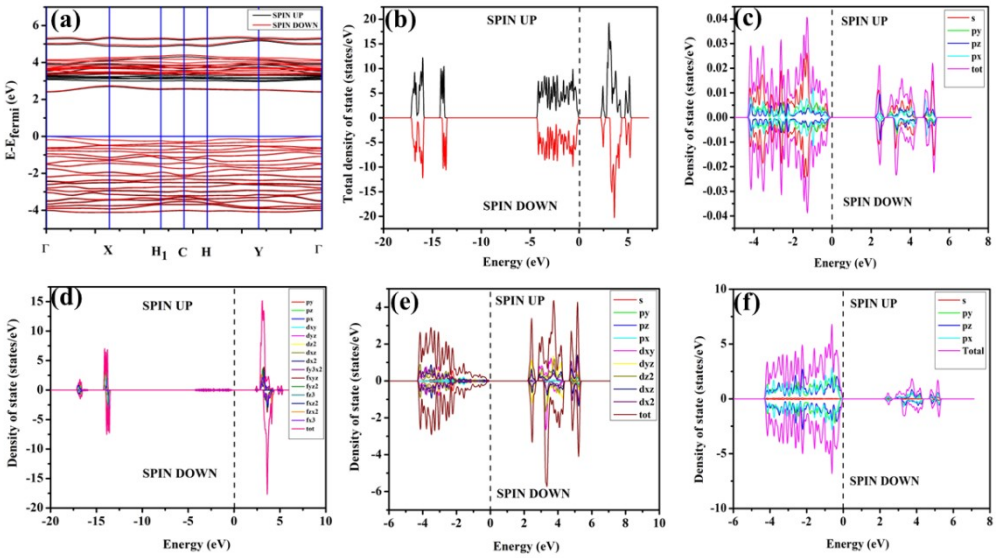

Fig. S17 (a) Band structure and (b) spin polarised TDOS and PDOS of (c) Na, (d) Ce, (e) Mo and (f) O of NCMO – $V_O^{\bullet}$.

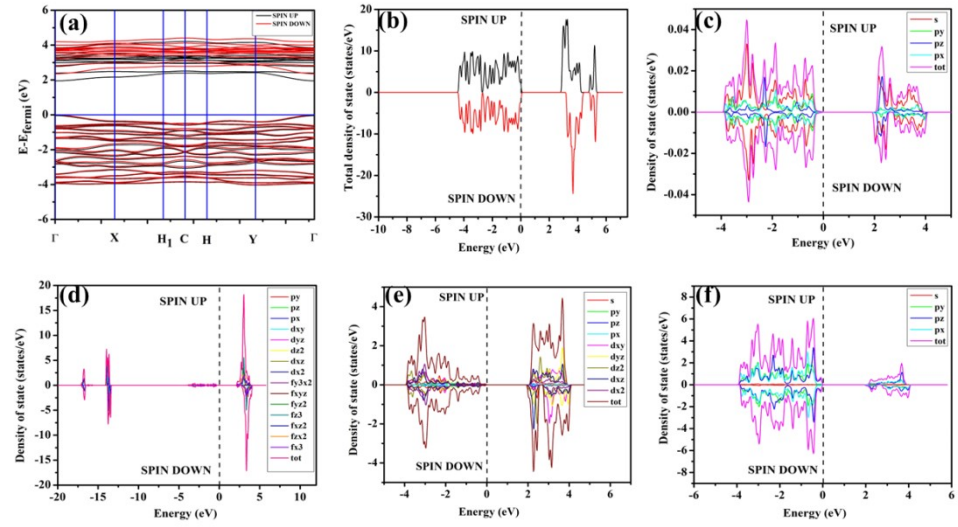

Fig. S18 (a) Band structure and (b) spin polarised TDOS and PDOS of (c) Na, (d) Ce, (e) Mo and (f) O of NCMO – $2V_O^{\bullet}$.

Calculation of $\varepsilon_c(1,3+, Ce^{3+})$

Presently, we have calculated shift of the centroid of according to eqn (1) [45].

$\varepsilon_c(1,3+, Ce^{3+}) = 6.35 - E^C(1,3+, Ce^{3+})$ (1)

And $\varepsilon_c(1,3+, Ce^{3+})$ is found to be 5.91, 5.67 and 5.43 eV for CeO_8, CeO_7 and CeO_6 respectively, therefore, red shift of the 5d – 4f transition is ascribed to reduce $\varepsilon_c(1,3+, Ce^{3+})$ in CeO_7 and CeO_6 with reference to CeO_8. In order to validate blue II emission with crystal field splitted d-orbitals or not, we have also calculated crystal field stabilization energy $\varepsilon_{cfs}(1,3+, Ce^{3+})$ using eqn (2)

$\varepsilon_{cfs}(1,3+, Ce^{3+}) = \beta R_{av}^{-2}$ (2)

where, $\beta = 1.35 \times 10^9$ pm^2 cm^{-1} for Ce^{3+} and $R_{av} = \frac{1}{N}\sum_{i=1}^{N}(R_i - 0.6\Delta R)$; R_i denotes individual bond lengths to the N coordinating anions in the un-relaxed lattice. We have obtained $\varepsilon_{cfs}(1,3+, Ce^{3+}) \sim 2.16$, 3.37 and 4.56 eV for CeO_8, CeO_7 and CeO_6 respectively indicating that splitting of d-orbitals of Ce^{3+} gradually increases from CeO_8 (~ 17,500 cm^{-1}) to CeO_6. Herein, we have noticed the difference between $^5D_0 - {}^2F_{5/2}$ and $^5D_0 - {}^2F_{7/2}$ transitions ~ 2,000 cm^{-1}, while blue I and blue II are differed by ~ 1082 cm^{-1}, hence blue II emission cannot be attributed to either $^5D_0 - {}^2F_{7/2}$ transition within CeO_8 polyhedra or 5d orbital splitted transition. Given that $2V_O$ gives two distinct $\varepsilon_c(1,3+, Ce^{3+})s$ within CeO_6 according to our DFT calculations, thus we ascribe blue II emission with other $\varepsilon_c(1,3+, Ce^{3+})$ (discussed later). It will be interesting to note from Fig. 4(e) that intensities of green and blue II gradually increase from $NCMO_{0.00}$ to $NCMO_{1.00}$, due to increase of $2V_O$ i.e. CeO_6 which agrees well with our FTIR, XPS results giving that $Na_3Cit.2H_2O$ has a predominant role to tune oxygen vacancy, especially $2V_O$.